Carbohydrate Polymers 196 (2018) 385–397

Contents lists available at ScienceDirect

Carbohydrate Polymers

journal homepage: www.elsevier.com/locate/carbpol

Comparison of nanocrystals and nanofibers produced from shrimp shell α-chitin: From energy production to material cytotoxicity and Pickering emulsion properties

Fatma Larbi[a,c,*], Araceli García[d], Luis J. del Valle[e], Ahmed Hamou[c], Jordi Puiggalí[e], Naceur Belgacem[a], Julien Bras[a,b,*]

[a] Univ. Grenoble Alpes, CNRS, LGP2, F-38000 Grenoble, France
[b] IUF, F-75000 Paris, France
[c] University of Oran 1 Ahmed Ben Bella, Department of Physics, Laboratory for Study of Environmental Sciences and Materials (LESEM), El M'naouar, Oran, Algeria
[d] University of Cordoba, Department of Organic Chemistry, Marie Curie Building C-3, Crta Nnal IV km 396, 14014 Cordoba, Spain
[e] Barcelona Research Center for Multiscale Science and Engineering, Departament d'Enginyeria Química, Escola d'Enginyeria de Barcelona Est (EEBE), Univ. Politècnica de Catalunya (UPC), c/Eduard Maristany 10-14, Barcelona 08019, Spain

ARTICLE INFO

Keywords:
Chitin nanocrystals
Chitin nanofibers
Pickering emulsions
Cytotoxicity
Energy cost

ABSTRACT

Chitin nanocrystals (ChNCs) and chitin nanofibers (ChNFs) are nanomaterials with great innovative potential for sustainable applications in academic and industrial fields. The research related to their isolation and production, characterization, and utilization is still new. The aim of this study is to investigate the effects of the production process on the morphology and properties of ChNFs and ChNCs produced from the same source of chitin. ChNCs were prepared by acid hydrolysis of commercial shrimp shell α-chitin, and ChNFs were prepared by mechanical defibrillation using closed loop supermass colloidal grinding. Differences in their shape, size, and crystallinity were observed. ChNFs were observed to have higher aspect ratio, higher viscosity, and better thermal stability than ChNCs. Although the ChNC casting film had a higher degree of transparency, it had lower mechanical properties than ChNF film. In addition, the capacities of each nanomaterial for producing Pickering emulsions were comparatively investigated. ChNFs showed better oil-in-water emulsion stabilization ability than ChNCs at the same concentrations. In vitro cytotoxicity assays using two epithelial-like cell lines and two fibroblast-like cell lines demonstrated that both nanomaterials were non-toxic. Finally, we evaluated the economics of production using process engineering simulation to assess the energy and chemical consumption for each process of production of these nanomaterials.

1. Introduction

Among the variety of renewable polymers, chitin is considered as one of the most abundant natural polymer on earth. The annual amount of chitin produced by biosynthesis—estimated between 10^{10} and 10^{11} tons—makes it the second most abundant biopolymer after cellulose (Gopalan Nair & Dufresne, 2003). Chitin, which is structurally similar to cellulose (Zhang, Chen et al., 2015; Zhang, Liu et al., 2015) is a linear polysaccharide that contains repeating units of β-(1 → 4)-N-acetyl-D-glucosamine, described for the first time in 1811 by Henri Braconnot (Muzzarelli et al., 2012). Chitin shares with cellulose the same fibrillar structure, which comprises both crystalline and amorphous components. In nature, three different polymorphic forms exist, differing in the orientation and arrangement of the macromolecular chains: α (the most abundant of the three forms, composed of alternating antiparallel chains), β (composed of parallel chains), and γ (the least common, composed of two parallel chains alternating with one anti-parallel chain) (Pereira, Muniz, & Hsieh, 2014).

Chitin is mainly produced by numerous living organisms through biosynthetic pathways. Generally, this polymer is a characteristic component of the exoskeletons of arthropods and the cell walls of fungi, and it is mostly associated with other compounds such as proteins, minerals, lipids, and pigments. Therefore, the most common industrial source for the production of chitin is mainly crab and shrimp shells from industrial seafood residues (Ding, Huang, Pang, Duan, & Zhang, 2018; Goodrich & Winter, 2007; Rinaudo, 2006).

In the current context, despite its enormous annual production and environmentally friendly aspects, such as biodegradability,

* Corresponding authors at: Univ. Grenoble Alpes, CNRS, LGP2, F-38000 Grenoble, France.
E-mail addresses: julien.bras@grenoble-inp.fr, julien.bras@pagora.grenoble-inp.fr (J. Bras).

https://doi.org/10.1016/j.carbpol.2018.04.094
Received 20 December 2017; Received in revised form 24 April 2018; Accepted 24 April 2018
Available online 25 April 2018
0144-8617/

biocompatibility, renewability, and sustainability (Ifuku & Saimoto, 2012; Lu et al., 2013), this biopolymer is still relatively underutilized. This is not only owing to its intractable bulk structure but also to its poor solubility in most solvents as a consequence of its micellar structure resulting from hydrogen bonds involving the aceto-amido groups (Garcia et al., 2015; Muzzarelli, 1983). This limits its potential applications compared to the other polysaccharides. Thus, developing new and efficient methods for better utilization of this natural resource is an active area of research.

In recent years, simultaneously with the exponential growth in the number of research projects on nanoscaled cellulose, the isolation and extraction of nanosized crystalline chitin, also called nanocrystals or whiskers, have attracted great interest. Moreover, recent developments have enabled the conversion of chitin into individual nanofibers as new flexible nanomaterials with high aspect ratios. The production of these nanomaterials is now the most efficient approach for exploring the potential of this biopolymer, giving rise to new applications. A wide variety of chitin nanocrystals (ChNCs) (Fan, Saito, & Isogai, 2008a, 2010; Gopalan Nair & Dufresne, 2003; Kadokawa, Takegawa, Mine, & Prasad, 2011; Li, Revol, & Marchessault, 1996; Paillet & Dufresne, 2001; Pereira et al., 2014; Revol & Marchessault, 1993) and chitin nanofibers (ChNFs) (Aklog et al., 2016; Fan, Saito, & Isogai, 2008b; Ifuku et al., 2009, 2011; Mushi, Butchosa, Salajkova, Zhou, & Berglund, 2014; Noh et al., 2006; Pang et al., 2017; Salaberria, Fernandes, Diaz, & Labidi, 2015; Wang, Yan, Chang, Ren, & Zhou, 2018) have been produced from different sources of chitin. The most conventional method for producing ChNCs is hydrolysis in a diluted acid solution of HCl under stirring at a high temperature (Paillet & Dufresne, 2001), whereas mechanical disintegration of chitin by simple wet grinding in the presence of minor amounts of acetic acid was more recently proposed (Ifuku et al., 2009), resulting in ChNFs.

Applications of such chitin nanomaterials in food, packaging, biological and biomedical fields are increasing owing to their renewable and biodegradable characteristics, nanoscale dimensions, low density, chemical stability, biological activity, and non-cytotoxicity (Salaberria, Fernandes, Diaz, & Labidi, 2015). Chitin nanomaterials have been used for interesting applications such as reinforcing nanofillers for various types of polymers (Butchosa et al., 2013; Deng, Li, Yang, & Li, 2014; Ji, Wolfe, Rodriguez, & Bowlin, 2012; Ma et al., 2016; Salaberria, Labidi, & Fernandes, 2014; Shankar, Reddy, Rhim, & Kim, 2015; Wu, Lin, & Meredith, 2016).They have also been utilized in electrospinning (Liu, Liu et al., 2016; Liu, Zheng et al., 2016; Zhu, Liang, & Ji, 2015), for preparation of water purification membranes (Ma, Burger, Hsiao, & Chu, 2011), and as alternative nanopaper membranes for biomedical and packaging applications (Ezekiel Mushi, Butchosa, Zhou, & Berglund, 2014). Other studies reported their application in tissue engineering, regenerative medicine, and wound dressing (Ito et al., 2014; Liu, Liu et al., 2016; Liu, Zheng et al., 2016; Muzzarelli et al., 2007; Pangon, Saesoo, Saengkrit, Ruktanonchai, & Intasanta, 2016).

Despite the growing scientific interest regarding other nanopolysaccharides, like nanocellulose, the literature on nanochitin is still limited. Indeed, over the last two decades, approximately 7070 documents (e.g., patents and scientific reports) on cellulose nanomaterials (between nanofibers and nanocrystals) were published, whereas only 664 documents on chitin nanomaterials were published during the same period from SciFinder database in 2017. This shows that chitin nanomaterials are still poorly utilized and that additional detailed analyses and investigations are needed to address its potential applications. In this context, this work intends to further characterize ChNCs and ChNFs produced from exactly the same source of chitin. The main idea is to understand how preparation conditions influence the structure and how the structure influences their properties. To our knowledge, Fan, Fukuzumi, Saito, & Isogai (2012) produced the only report prior to this one that compares the properties of these two chitin nanomaterials in the same work; they compared the properties of dispersions of nanochitin prepared by different methods and from different sources. We note that in their study, the comparison was between nanocrystals from crab shell α-chitin and nanofibers from squidpen β-chitin. In contrast, we compared the properties of these two nanomaterials from the same source—shrimp shell α-chitin, the most abundant and stable form of chitin (Chen, Shen, & Liu, 2010; Kumirska et al., 2010). Furthermore, the ability to produce Pickering emulsions with these two nanomaterials, which has never been the subject of comparative investigation, was explored. Additionally, the possible in vitro cytotoxicity of these nanomaterials was tested against two epithelial-like cell lines and two fibroblast-like cell lines. Moreover, the mechanical fibrillation of chitin using a closed loop grinding process was analyzed by process engineering simulation to quantify the energy necessary for fibrillation and to compare it with the process energy for ChNC isolation. This aspect has not been investigated before; therefore, this work provides basic data for more detailed studies on this topic.

2. Material and methods

2.1. Materials

Coarse flakes of α-chitin from shrimp shells with a degree of acetylation DA ≥ 95%, hydrochloric acid (concentrated 37% v/v), sodium acetate, glacial acetic acid, potassium hydroxide, sodium chlorite, and sodium chloride were purchased from Sigma Aldrich (France). Sunflower oil was obtained from a local supermarket and used without further purification. All chemicals were used as received.

2.2. Preparation of chitin nanomaterials

2.2.1. Purification step of chitin

The isolation processes of the nanosized materials are illustrated in Fig. 1. Before their isolation, chitin was subjected to a purification step in order to eliminate proteins. A 40-g sample of chitin was initially heated for 6 h in 5% KOH solution at 100 °C (900 mL). Subsequently, it was mechanically agitated overnight at room temperature; the following day, it was washed and vacuum-filtered several times with distilled water. Bleaching was performed in two cycles of 2 h, each one at 80 °C in a solution of 17 g of $NaOCl_2$ in 1 L of 0.3 M sodium acetate buffer, pH 4. The material was then placed again in a solution of 5% KOH for 48 h to remove any protein residues still present in the material, followed by another cycle of vacuum filtration and washing with distillated water. This purified chitin—henceforth referred to as p-Chitin—was used as the raw material for the rest of study.

2.2.2. ChNC preparation

ChNCs were prepared following a previously used method (Gopalan Nair & Dufresne, 2003). The p-Chitin was hydrolyzed in 3 M HCl for 90 min at 90 °C to digest the disordered regions—the ratio of 3 M HCl solution to chitin was 30 mL/g. Afterwards, the material was diluted with distilled water and collected for centrifugation at 10000 rpm for 15 min at 4 °C. This process was performed three times. Then, the material was dialyzed in membranes (MWCO 6000-8000 Da) and kept in distilled water for five days to reach a pH of 5–6. The suspension was subjected to ultrasonic treatment for further dispersion of the ChNCs, and the product was finally stored at a temperature near 4 °C after adding 3 drops of chloroform to avoid bacterial growth. The ChNC dispersion was determined gravimetrically by drying aliquots of the sample at 105 °C until a constant weight was obtained; the total solid content of the stock dispersion was approximately 3.4 wt%.

2.2.3. ChNF preparation

ChNFs were prepared from never-dried p-Chitin under acidic conditions according to the procedure of Ifuku et al. (2009). The p-Chitin was suspended in distilled water at a concentration of 1%. The suspension was acidified by addition of acetic acid to adjust the pH to 3 for cationization of amino groups on the fiber surface to enhance

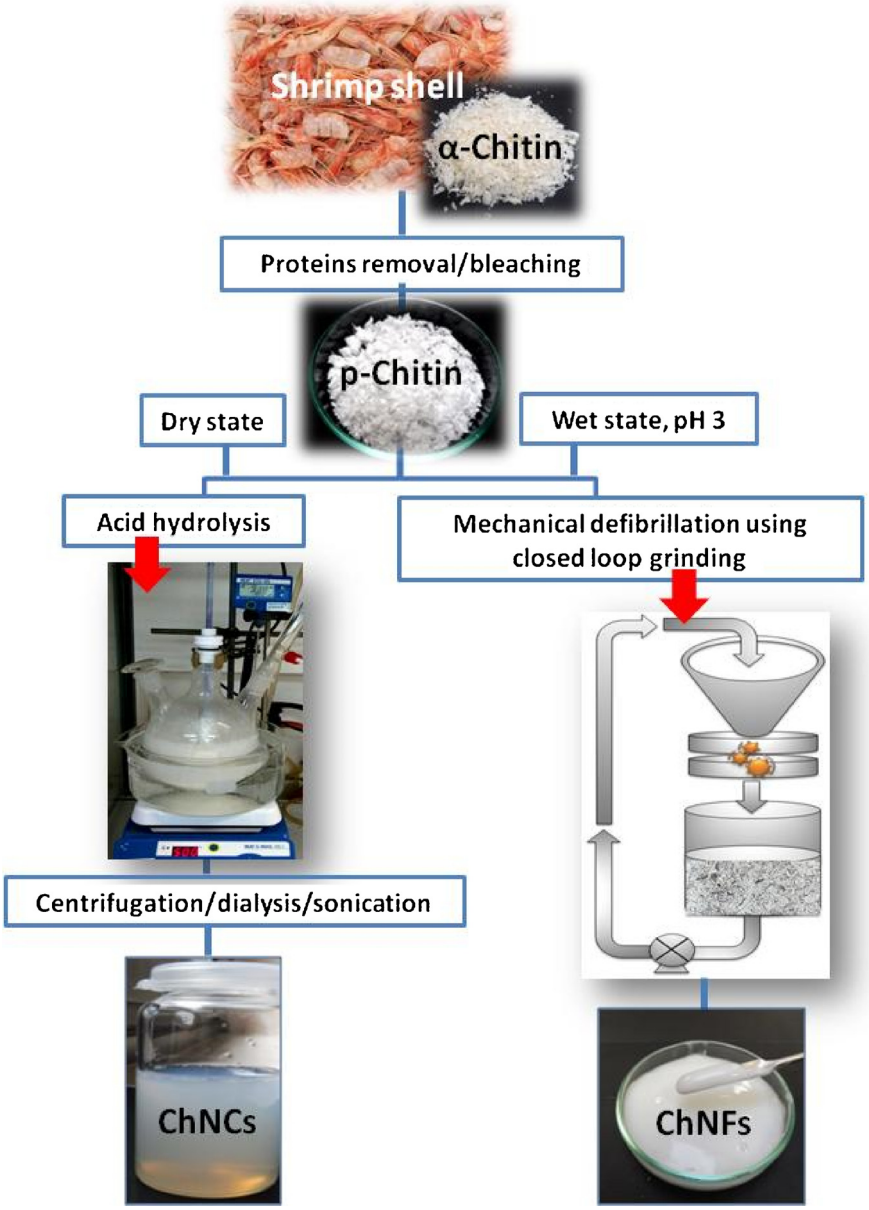

Fig. 1. Simplified experimental procedure for production of ChNCs and ChNFs from shrimp shell chitin.

nanofibrillation by exerting an electrostatic repulsive force. It was then blended with a high-speed kitchen blender for 10 min. The slurry was then passed through an ultrafine friction grinder (Supermasscolloider, model MKZA6-2, disk model MKG-C 80, Masuko Sangyo Co., Ltd., Japan) at 2500 rpm under continuous fibrillation for 3 h. Grinder treatment was performed with a clearance gauge of −1.5 (corresponding to a 0.15 mm shift) from the zero position and a recirculation loop device. The obtained ChNF dispersion was concentrated by centrifugation to eliminate as much water as possible, yielding a 2.6 wt% stock dispersion, which was stored at 4 °C.

2.3. Film preparations of ChNCs and ChNFs

Preparation of films was performed using a casting process. Fixed amounts of 1 wt% ChNC and ChNF suspensions were poured onto Teflon plates and dried under ambient conditions for 7 days until the films formed; afterwards, they were conserved in a conditioned room, under controlled temperature (23 °C) and relative humidity (50%).

2.4. Emulsion preparation

Oil-in-water emulsions were prepared by mixing appropriate quantities of ChNC or ChNF stock dispersions with sunflower oil. The aqueous dispersions were previously adjusted to pH 3.0 before mixing with the emulsion. The oil–water mixture was then emulsified using an ultra-turrax homogenizer for 5 min at 10000 rpm and 1 min at 15000 rpm. The sunflower oil concentration was maintained at 20 wt% of the total weight of emulsions, while the ChNC and ChNF concentrations were varied from 0.1 to 1.4 wt%. The emulsions were placed in small transparent vials for several days to observe their evolution.

2.5. Techno-economic evaluation of chitin nanomaterial production processes

To roughly analyze the economic issues of the ChNC and ChNF production processes, a preliminary evaluation of mass and energy balances was performed. All the steps described in Sections 2.1–2.2

were considered for this objective. The economic assessment was evaluated using the process simulation tool Aspen Plus (AspenTech, Virginia), following similar methodology to that described previously (Novo, Bras, García, Belgacem, & Curvelo, 2015). Traditional chemical components (i.e., water, potassium hydroxide, sodium acetate, sodium chlorite, hydrochloric acid, acetic acid) were defined using the available Aspen properties database. Regarding chitin definition, its basic physicochemical properties and thermodynamic behavior were assumed from data available for cellulose in the same database, as these two polysaccharides have similar main structure and properties.

The operation basis was established for 1 kg of initial chitin that was first purified. The chemicals requirements and yield of the different designed pretreatments were considered from the aforementioned experimental procedure and from the gravimetric product changes registered throughout chitin nanomaterial production. Energy consumption during purification was assumed to be due to (1) pretreatment heating (determined from designed simulation) and (2) mechanical treatments (estimated from experimental or literature data). The energy consumption for the chitin nanofibrillation process in the ultrafine grinder was calculated as the product of experimentally consumed power P (kW) and the process duration t (h). A detailed description of the simulation process is given in Supplementary Data.

2.6. Measurement and characterization

2.6.1. Atomic force microscopy (AFM) measurements

AFM images of nanodispersions and the surface of their films casting were obtained using a Multimodal AFM (DI, Veeco, Instrumentation Group) operating in the tapping mode. Approximately 0.01 wt% suspensions were drop-deposited on a mica substrate and allowed to air dry before image acquisition. At least 50 images from three micrographs were used to perform dimension calculation. For AFM images of the film surfaces, 0.5 cm^2 of each film was stuck on the mica substrate.

2.6.2. Scanning electron microscopy (SEM)

SEM images of the fractured surface of casting films of ChNCs and ChNFs were obtained by cooling each sample in liquid nitrogen and fracturing them. The surface morphology of the films was also characterized by this technique. The micrographs were recorded with a QUANTA 200 instrument operating at an accelerating voltage of 10 kV. A minimum of 10 images by samples were collected. The SEM images selected for the figures are the most representative of the samples.

2.6.3. Field emission gun (FEG)-SEM

Chitin nanodispersions were also observed by FEG-SEM which was performed using a ZEISS Ultra 55 microscope, equipped with an In-Lens secondary electron detector. An accelerating voltage of 3 kV was used. Preparation of the samples was the same as for AFM measurements. The FEG-SEM images selected for figures are the most representative of the samples.

2.6.4. X-ray diffraction (XRD) analysis

The crystallinity (referred to as the crystallinity index) of Chitin, p-Chitin as well as dry ChNC and ChNF powders was determined from wide-angle XRD spectra. XRD patterns of the chitin samples were recorded in a range of 2θ from 6° to 55° with the reflection mode in a classical Bragg–Brentano geometry at room temperature using a PANalytical X'Pert Pro MPD diffractometer equipped with an X'celerator detector and operated with CuKα radiation with a wavelength of 1.5419 Å. Analysis of the XRD data was performed with the PeakFit v4 software (Jandel Scientific Software). Thus, the diffraction data were deconvoluted and fitted with Gaussian-Lorentzian line shapes to identify the crystalline and amorphous contributions. The accepted models had a correlation coefficient > 0.98.

2.6.5. Thermogravimetric analyses (TGA)

The thermal stability of the stock chitin nanomaterials was also studied. Measurement was performed on a PerkinElmer Simultaneous Thermal Analyzer (STA 6000). The samples were tested with a heating rate of 10 °C/min from ambient temperature to 700 °C under 50 mL/min flow of nitrogen atmosphere. The reproducibility was confirmed by performing duplicate measurements. The samples' weights were approximately between 5 and 10 mg.

2.6.6. Mechanical properties

Tensile tests were conducted at a speed of 0.001 mm/s using an RSA3 (TA Instruments, USA). The elongation, stress at break, and the Young's modulus were determined. The samples were previously conditioned for at least 72 h under controlled temperature (23 °C) and relative humidity (50%), before being tested. These measurements were performed at least in triplicate, and the reported values are the averages.

2.6.7. Rheological properties

For the rheological measurements, two different concentrations of each nanochitin dispersion were prepared by diluting the concentrated dispersions with distilled water until reaching 1 wt% and 2 wt%. Rheological measurements of the suspensions were made using a Modulating Compact Rheometer ANTON PAAR with measuring cone geometry CP50-1 (cone angle, 1°; diameter, 50 mm) at 25 °C. For each sample, an "up–down" shear-rate cycle was conducted from 10 s^{-1} to 1000 s^{-1} with considering stable value in each case. Only the "down" parts of the curves are presented in this work. The ChNF suspensions were dispersed in advance for 2 min by the ultra-turrax, whereas the ChNC suspensions were dispersed in advance for 2 min by sonication. Duplicate measurements were performed to confirm reproducibility.

2.6.8. Visual inspection of emulsion stability

We monitored the evolution of the sunflower oil volume fraction in the vials by photographing them at different time intervals over 42 days. Digital photos were taken using a Panasonic digital camera at different intervals of time against a dark background. The objective was observing the gravitational separation in the emulsions. In general, it is possible to visually detect two layers after creaming has occurred: a lower serum optically transparent layer and an upper opaque cream layer. The extent of creaming was characterized by a creaming factor (CI), defined as (Mwangi, Ho, Tey, & Chan, 2016):

$$CI\% = (H_S/H_E) \times 100, \quad (1)$$

Where H_S is the height of lower serum layer and H_E is the total height of the emulsion in the vial. At least two samples of each emulsion were prepared to confirm results.

2.6.9. Cytotoxicity assay

The cytotoxicity assay was performed by evaluating ChNC and ChNF extracts using two epithelial-like cell lines (Madin Darby canine kidney, MDCK cells; and Madin Darby canine kidney-sialic acid over expression, MDCK-SIAT cells) and two fibroblast-like cell lines (*Cercopithecus aethiops* kidney, Cos-1 and Cos-7 cells). For ChNFs, we prepared the suspension in advance by acid removal via dialysis in distilled water until reaching neutrality.

The extracts were prepared by suspending 1 g of ChNCs or ChNFs in 10 mL of Dulbecco's Modified Eagle Medium (DMEM) supplemented with 100 U/mL penicillin, 100 μg/mL streptomycin, and 10%-v/v fetal bovine serum. The suspensions were homogenized in 15 mL Falcon tubes using a vortex mixer and then incubated in culture conditions for 24 h at 37 °C and 5% CO_2 in air. Then, the extracts were sterilized by filtration using a membrane with a pore size of 0.22 μm; this operation was performed in a laminar flow cabinet.

Cells for the assay were seeded into 96-well culture plates at a

density of 10^4 cells/well and the plates were maintained in culture conditions to allow adhesion and monolayer formation. After 24 h, the media were aspirated and the cells were exposed to different concentrations of the ChNC and ChNF extracts; in all cases, the medium/extract volume was 100 µL per well, and the plates were maintained in culture for 24 h. Each concentration of the extracts and the zero-concentration (control) were assayed in triplicate. Finally, the cell morphology was evaluated by optical microscopy to evaluate possible cytopathic effects, and cytotoxicity was quantified by the MTT assay. For this assay, the media were aspirated and the cells were washed three times in PBS and then incubated with 100 µL of MTT reagent (5 mg/mL MTT was dissolved in fresh medium) for 3 h to allow the formation of formazan crystals in the viable cells. Their quantification was performed by solubilizing them in a DMSO/methanol/water mixture (20/70/10, %-v), and the absorbance at 570 nm was determined using a microplate reader (Biochrom, UK).

2.6.10. Statistical analysis

Data are expressed as mean ± SD, and statistically tested for significance with one-way ANOVA followed by a Tukey test using OriginPro v10 software (Origin Microcal, USA), and $p < 0.05$ was considered statically significant.

3. Results and discussions

3.1. Difference in chitin nanomaterial structures and morphology

The distributions of the widths and lengths of the ChNC and ChNF samples were obtained by analysis of the AFM and FEG-SEM height images (Fig. 2). Length-frequency figures were obtained from the combined AFM and FEG-SEM observations using ImageJ while width-frequency figures resulted from AFM observation using Nanoscope Analysis (Plainview, New York, USA). ChNCs and ChNFs had similar geometric forms with different size dimensions. ChNCs and ChNFs presented rod-like morphology and were well individualized with some aggregates or nanofibrillar structures bounded together. In some cases, the aggregation of these materials has been explained by the presence of protein residues on the surface of the chitin (Paillet & Dufresne, 2001). For ChNCs, ultrasound treatment can also be performed to ensure complete individualization of the ChNCs, which is enhanced by electrostatic repulsion between some ChNCs improved by the presence of positive charges (NH_3^+) on their surfaces. However, the resulting ChNC dispersion obtained after dialysis treatment had a pH of approximately 6; at this pH, the amount of protonated amino groups is not sufficient to bring about electrostatic repulsion between ChNCs, which can lead to the formation of agglomeration even after ultrasonication. According to some reports, it is recommended to first adjust the pH of the dialyzed chitin suspension at 3 or below to ensure complete protonation of the accessible surface amino groups followed by ultrasound treatment (Li, Revol, Naranjo, & Marchessault, 1996).

The length dimensions of ChNCs ranged from 229 nm to 258 nm, with an average value of (243.5 ± 55.1) nm, whereas the width mostly ranged from 9 nm to 10 nm, with an average value of (9.7 ± 3.2) nm. These values are in the intervals found in previous studies performed on different origins of chitin based on the same procedure of preparation; the obtained ChNCs had lengths ranging from 150 nm to 2200 nm and widths ranging from 10 to 50 nm (Zuber, Zia, & Barikani, 2013). However, it is important to note that reaction conditions can generate various size distributions of ChNCs even from the same source of chitin (Table 1).

contrast, the ChNFs prepared using mechanical treatment had widths ranging from 8 nm to 9 nm with an average value of (8.7 ± 3.2) nm, and they were longer than the ChNCs, with a length mainly distributed between 604 nm and 744 nm and an average value of (673.9 ± 263.3) nm. This evinces the fact that the aspect ratio—defined as the length to width ratio—of ChNFs is higher than that of ChNCs. We note that there are no prior reports on the preparation of ChNFs from shrimp shells using the same mechanical procedure. This difference in the morphological appearance and size between the resulting chitin nanomaterials will allow us to accurately evaluate how the treatment process would influence the other properties.

The crystalline structure of chitin samples was investigated using XRD. As shown in Fig. 3(a), the native chitin exhibited diffraction peaks at 9.3°, 12.8°, 19.4°, 20.7°, 23.4°, and 26.5°, which are typical crystalline patterns of α-chitin, corresponding to the (020), (021), (110), (120), (130) and (013) planes, respectively (Goodrich & Winter, 2007; Ifuku, Suzuki, Izawa, Morimoto, & Saimoto, 2014). The observed patterns show that the chemical treatment of purification and the subsequent acid hydrolysis or mechanical process during the formation of ChNCs or ChNFs, respectively, did not alter the crystalline arrangement of α-chitin. Moreover, by comparing the X-ray diffraction patterns, the intensity of the major crystalline diffraction peak at 19.4° clearly increased after the indicated treatments, which is due to the increase in crystallinity after removing the amorphous parts.

The Crystallinity Index (CrI) of the chitin samples was calculated as the ratio of the areas of all crystalline reflections to the total area. Therefore XRD data were deconvoluted as shown in Fig. 3(a). A total of 12 individual crystalline peaks were extracted by a curve-fitting process from the X-ray diffraction profiles over the range of measurements. Two amorphous halos were approximately estimated using two broad maxima. The first maximum observed at lower diffraction angles (at 2θ–21.5°) resulting from the intermolecular scattering and the second one observed at higher angles (at 2θ–41.5°) resulting from intramolecular scattering (Stawski, Rabiej, Herczyńska, & Draczyński, 2008). The obtained CrIs of the Chitin, p-Chitin, ChNFs, and ChNCs were 69.9%, 70.7%, 76.1% and 80.8%, respectively. ChNCs have the higher degree of crystallinity owing to the acidic hydrolysis process, which was more effective than mechanical treatment at substantially eliminating the entire amorphous remaining after purification. This result was expected. Overall, the high crystallinity index of both ChNCs and ChNFs indicates the conservation of the crystalline integrity of ChNFs and ChNCs even after mechanical and acid hydrolysis treatments, respectively.

TGA is used to measure the weight loss of a material as a function of temperature for a given heating rate. Fig. 3(b) shows the thermal stability of native α-chitin before and after purification with as-prepared ChNFs and ChNCs. All the samples showed initial light weight loss in temperatures ranging from 0 °C to 110 °C, which can be linked to water loss due to evaporation. The second and most significant weight loss occurred at 250 °C to 450 °C for all samples, which could be attributed to degradation of the chitin chain resulting from degradation of the saccharide structure of the molecule, dehydration of saccharide rings and the decomposition of acetylated and deacetylated chitin units (Shankar et al., 2015). The total weight loss in those ranges was approximately 80%, 83%, 83.5%, and 69% for Chitin, p-Chitin, ChNFs, and ChNCs, respectively. At higher temperatures (> 450 °C) the weight loss was attributed to the decomposition of remaining materials, which were more thermally stable structures, and char. Comparing ChNFs and ChNCs, we note that the thermal degradation of ChNCs started earlier at approximately 250 °C with a higher char value than that of ChNFs, which started decomposing at approximately 270 °C, indicating that ChNFs were more thermally stable than ChNCs. It is reported that this difference is related to the difference in their particle size; in fact, ChNCs have a smaller particle size with a high specific surface area, which implies the presence of a higher number of free end chains on the surface, promoting decomposition at lower temperatures (Zeinali, Haddadi-Asl, & Roghani-Mamaqani, 2014). The final residues of chitin, p-chitin, ChNFs, and ChNCs at 600 °C were 16.6%, 14.4%, 13.4%, and 25.9%, respectively. The highest residual mass of ChNC sample can be explained by the presence of some mineral traces due to the introduction of inorganic ions of Cl^- into crystalline chitin during acid hydrolysis that can act as a flame retardant. Furthermore, the decomposition

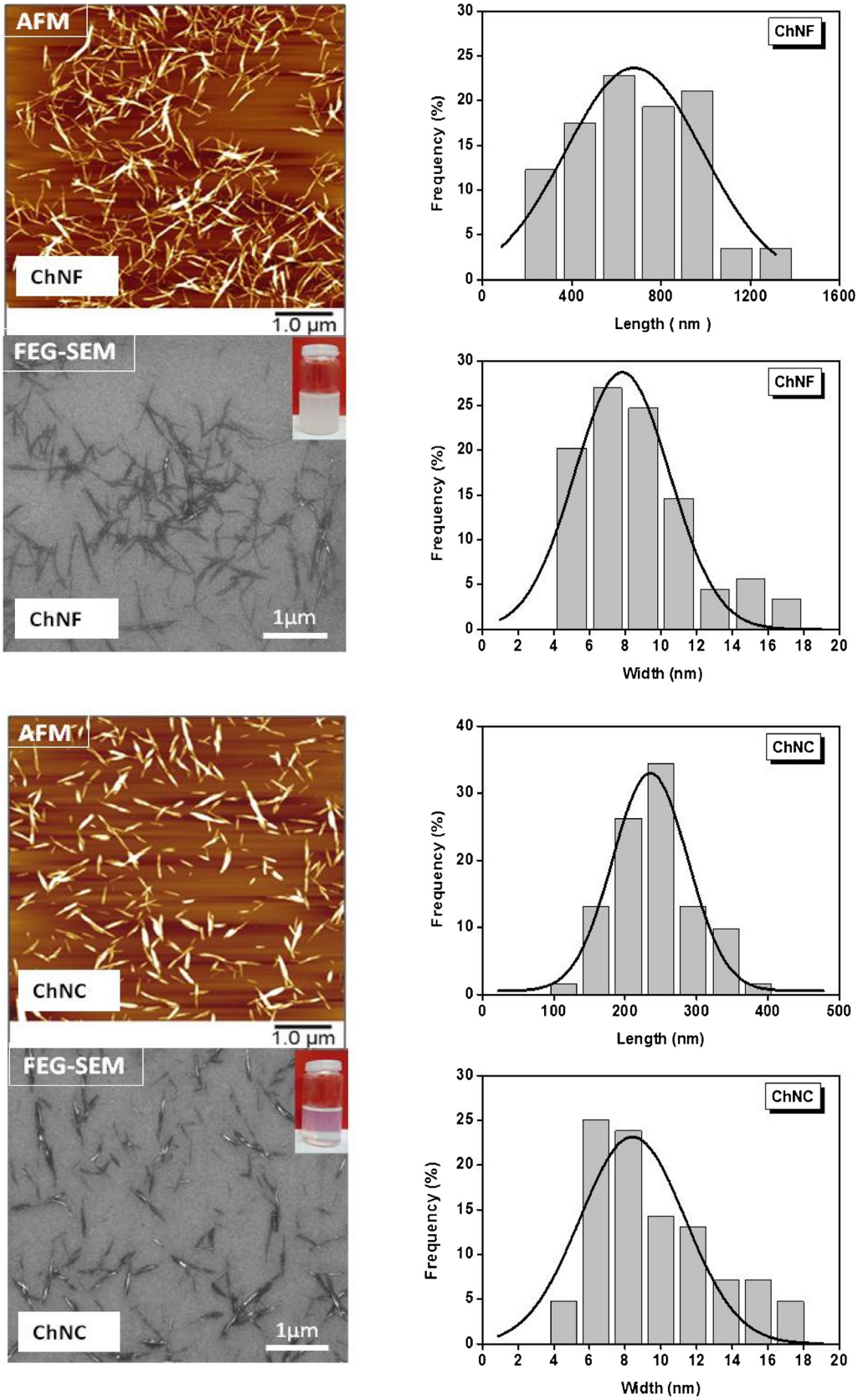

Fig. 2. AFM and FEG-SEM images of ChNFs and ChNCs with their length and width distributions.

Table 1
Sizes of ChNCs prepared from shrimp shell chitin with acid hydrolysis in 3 M HCl.

Length (nm)	Width (nm)	Hydrolysis conditions	Reference
■ 200–560	18–40	3 h at 105 °C	Phongying, Aiba, and Chirachanchai (2007)
■ 307.7	27.1	6 h at 104 °C	Ang-atikarnkul, Watthanaphanit, and Rujiravanit (2014)
■ 150–800	5–70	1.5 h × 3 at 104 °C and sonication	Sriupayo, Supaphol, Blackwell, and Rujiravanit (2005)
■ 100–500	5–80	1.5 h × 3 at boiling temperature and sonication	Gopi, Pius, and Thomas (2016)
■ 182 ± 91	9 ± 3	2 h at 105 °C and sonication	Butchosa et al. (2013)
■ 200–500	10–15	1.5 h × 3 at 90 °C and homogenization	Goodrich and Winter (2007)
■ 160 ± 77	16 ± 5	1.5 h at boiling temperature and sonication	Perrin, Bizot, Cathala, and Capron (2014)
■ 229–258 (243.5 ± 55.1)	9–10 (9.7 ± 3.2)	1.5 h × 3 at 90 °C and sonication	This study

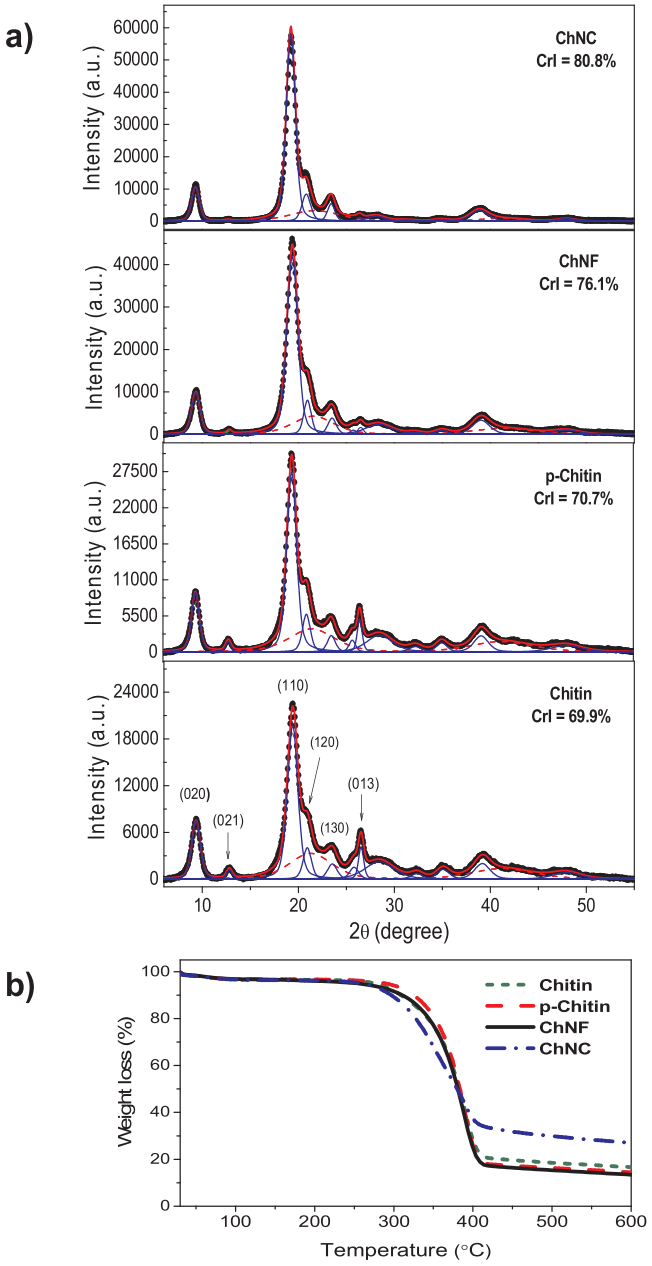

Fig. 3. (a) X-ray diffraction patterns (black dotted lines) of chitin samples; Deconvoluted amorphous halos (red dached lines) and crystalline peaks (blue lines) are indicated together with the corresponding simulated profile (red line). (b) TGA curves of Chitin, p-Chitin, ChNCs and ChNFs. (For interpretation of the references to colour in this figure legend, the reader is referred to the web version of this article.)

of the free end chains of ChNCs, resulting from acid hydrolysis, at lower temperature can consequently cause an increase in the final residues of these nanomaterials (Julien, Chornet, & Overend, 1993; Rahimi, Brown, Tsuzuki, & Rainey, 2016). Another argument can be related to the crystallinity; in fact, since the crystalline phase in ChNC sample is the highest compared to the other samples and considering that the material with higher crystallinity is more stable and more resistant to decomposition at high temperature than an amorphous material, therefore the weight loss of the residual part of ChNCs will be less important than those of the other samples whose initial weight contains more amorphous part which is more sensitive to decomposition under pyrolysis at high temperature.

3.2. Influence of treatment process on chitin nanomaterial film properties

To obtain more information about the morphology of the studied nanomaterials, cast films prepared by air-drying the suspensions in Teflon molds were analyzed using microscopy techniques. The surface morphologies of ChNF and ChNC films were observed by AFM using the tapping mode. As shown in Fig. 4, there are clear differences between the two films. The ChNF film shows ChNFs randomly distributed and forming aggregates (Fig. 4(a)). In contrast, in the ChNC film, individualized and well-dispersed ChNCs are seen forming aligned domains (Fig. 4(b)). This result is in excellent agreement with that of Fan et al. (2012).

Li et al. (2016) reported that in general, ChNCs are randomly distributed in the isotropic region and are almost completely organized in the anisotropic region. The photographs in the insets of Fig. 4 show that the two prepared films had different appearances even by visual inspection. The aqueous ChNC dispersion yielding a transparent and smooth surface film was obtained by casting (Fig. 4(b), inset); in comparison, the ChNF film appeared opaque with a rough surface (Fig. 4(a), inset).

The microstructure of the ChNC and ChNF films was further observed from the surface and fracture morphology by SEM. As shown in Fig. 4, the surface morphology of the films is in good agreement with those observed from AFM images. A rough surface with a clear composition of disordered ChNFs was observed in the ChNF film (Fig. 4(c)). In contrast, the ChNC film showed a smooth surface because of the order and bi-dimensional distribution of the ChNCs (Fig. 4(d)). Cross-section micrograph of the ChNC film (Fig. 4(f)) shows that it is more tightly packed together than the ChNF film (Fig. 4(e)). In contrast, the ChNF film showed numerous cavities that may be explained by the network formed by the over-lapped ChNFs. Indeed, contrary to the ChNCs, the ChNFs are flexible and can become entangled with each other.

The mechanical properties (Young's modulus, strength, and elongation at break) of such nanochitin films were also investigated at room temperature. The results are shown in Fig. 5. The ChNF film had higher tensile strength and elongation at break than the ChNC film; such results support the notion that the high aspect ratio and entanglement of ChNFs, which were much higher than those of ChNCs, had an important effect on the mechanical characteristics of the nanochitin films. It has

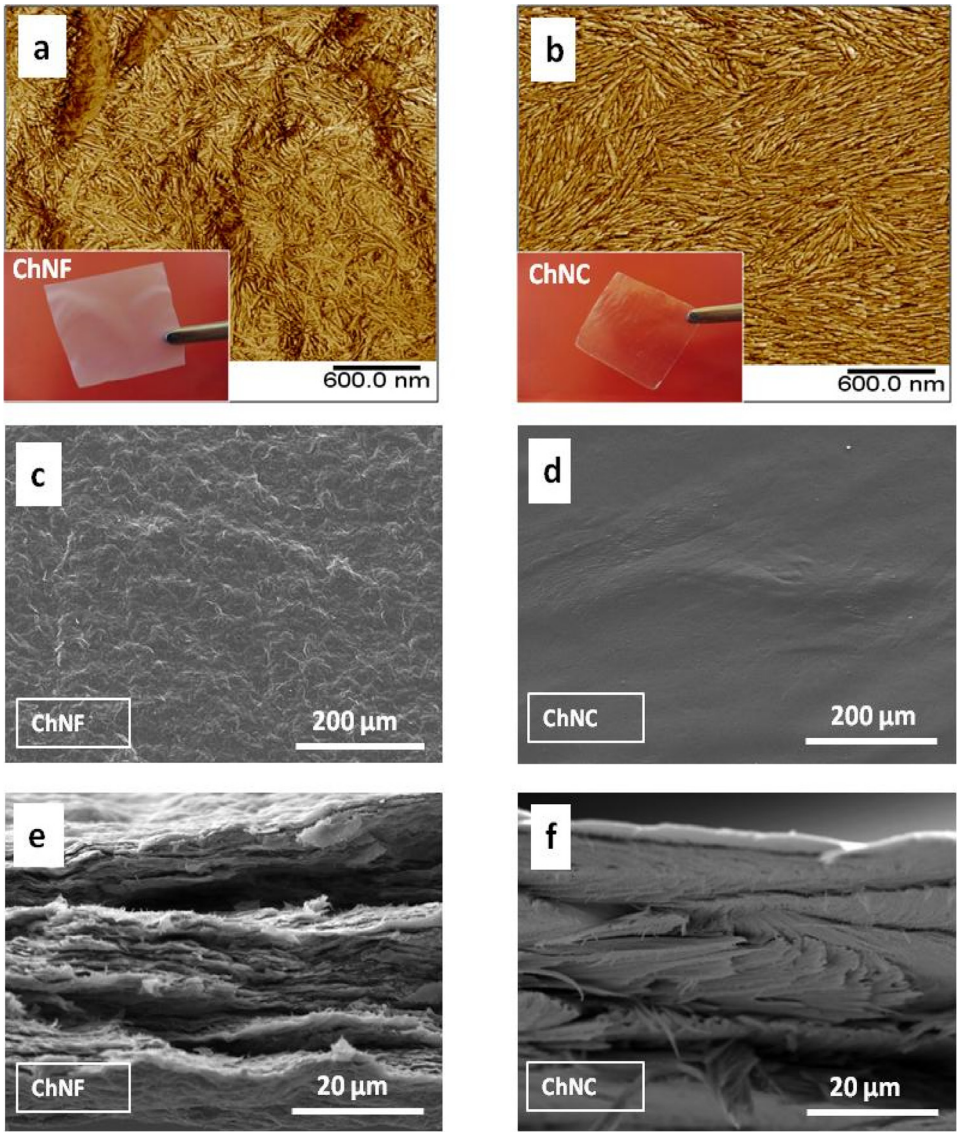

Fig. 4. AFM images of self-standing film surfaces of (a) ChNFs and (b) ChNCs. SEM images of nanochitin films of (c,d) surface and (e,f) fracture section in (c,e) ChNF film and (d,f) ChNC film.

been reported that large aspect ratios are beneficial for the formation of a strong and entangled network, leading to the superior reinforcement capacity of nanofillers in different polymer matrices while simultaneously avoiding the premature rupture of some polymers (Li et al., 2016). The large difference between the elongations at break of the two films is mainly related to the entanglement, nanoporosity, and

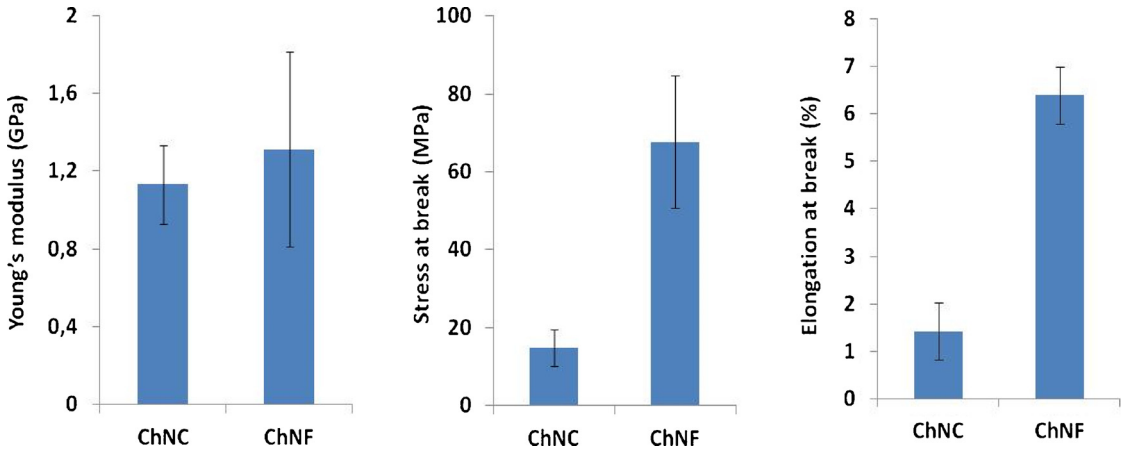

Fig. 5. Mechanical properties of nanochitin films.

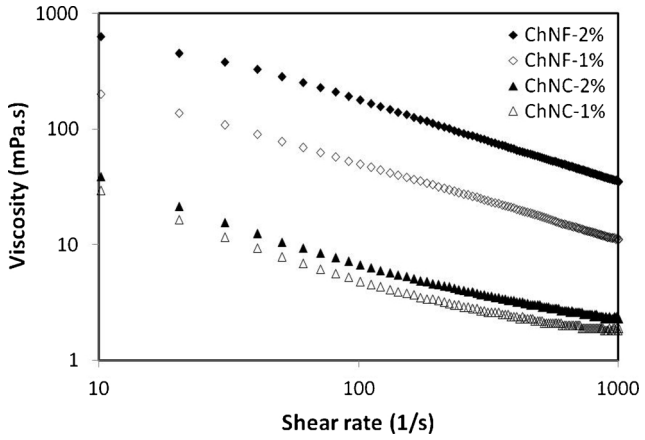

Fig. 6. Viscosity versus shear rate for ChNF and ChNC suspensions at two different concentrations.

close interaction between the nanomaterials, which occurs during the formation of each film. In contrast, there was no significant difference between the Young's moduli of the two films. The Young's modulus of ChNFs found in the current study ~1.31 GPa was very close to a previous result (Ifuku et al., 2012), which was 1.80 GPa, whereas the tensile strength of the ChNF film of this study ~67.7 MPa was much greater than that reported by Ifuku et al. (30 MPa). This result is probably due to the different conditions of mechanical tests—measured at 0.06 mm min^{-1} in the current study and 1.0 mm min^{-1} in the cited study. Additionally, the origin of chitin and the preparation of ChNF film used by Ifuku et al. were completely different from that of ours. Ifuku et al. prepared their ChNF films from crab shell chitin using a filtration process under reduced pressure, whereas we prepared our films from shrimp shell chitin using a solvent casting process. However, there are few reported studies about the mechanical properties of ChNC films. In this study, the Young's modulus and tensile strength were smaller than those reported earlier (Fan et al., 2012); whose Young's modulus and tensile strength of the ChNC film prepared from crab shell α-chitin were (5.7 ± 1.6) GPa and (49 ± 4.6) MPa, respectively.

3.3. Rheological properties of nanochitin suspensions

The viscosity is another important parameter that can be affected by the morphology of chitin nanomaterials. Fig. 6 shows the plots of viscosity versus shear rate for ChNF and ChNC suspensions at two different concentrations: 1 wt% and 2 wt%. The ChNF and ChNC suspensions had the same rheothinning tendency: the viscosities of the suspensions decrease with the increase of shear rate and with the decrease of concentration for the two nanodispersions; however, this fact was more visible for the ChNF suspension. In addition, the viscosity difference between the two different concentrations of ChNFs was higher than the difference observed for ChNCs.

Moreover, a large difference was observed between the viscosities of ChNF and ChNC suspensions. Indeed, the viscosity of the ChNF suspension was remarkably higher than that of the ChNC suspension at the same concentration throughout the range of the shear rates studied. This link to the higher flexibility and aspect ratio resulted in more intense percolation at similar concentrations. Zhang, Chen et al. (2015) and Zhang, Liu et al., (2015) also reported that such result is explained by the difference between the aspect ratios of the two nanomaterials, which has an important impact on the viscosity. In addition, Li, Revol, Marchessault et al. (1996) mentioned that the rheological properties of a suspension are also influenced by the inter-particle dispersion forces and electrostatic repulsive forces. Thus, these results demonstrate that viscosities of chitin nanodispersions are strongly dependent of the morphology and size of the nanomaterial.

3.4. Pickering emulsions

Emulsions are of considerable practical interest because of their extensive applications in many medical and pharmaceutical preparations, food, cosmetics, petroleum products, road construction and maintenance techniques, and agriculture (Chappat, 1994; Tzoumaki, Moschakis, Kiosseoglou, & Biliaderis, 2011). Emulsions are systems consisting of dispersed droplets of one liquid in another in which it is not soluble or miscible (Cunha, Mougel, Cathala, Berglund, & Capron, 2014; McClements, 2007). One of the most important properties of an emulsion that has direct impact on its application in many industrial products is its stability, which is defined as its ability to resist changes in its physicochemical properties overtime (McClements, 2007). Recently, it was shown that cellulose nanocrystals are good candidates for Pickering emulsions, emulsions where a solid phase exists at the interface between water and oil (Kalashnikova, Bizot, Bertoncini, Cathala, & Capron, 2012; Laitinen, Ojala, Sirviö, & Liimatainen, 2017; Wang et al., 2016).

In this study, we investigated the preparation and characterization of sunflower oil-in-water emulsions stabilized by ChNCs and ChNFs, referred to as Pickering emulsions. The emulsion characterization was performed by visual observation. The objective was to have a preliminary idea about the influence of ChNCs and ChNFs—with their different shape and morphology—on the stability of emulsions formulated with them and to simultaneously try to perform a comparative study between the two Pickering emulsions. As stated previously, the ChNC and ChNF concentrations were varied from 0.1 to 1.4 wt% of the total weight of the emulsions. Fig. 7 shows the CI plotted as a function of aging time over 42 days for all emulsions. It is clear that the CI depends on the time at which the measurement is made. The CI of ChNF and ChNC emulsions increased quickly to reach a plateau only a few days after preparation (Fig. 7(a) and (b), respectively). The increasing concentration of chitin nanomaterials reduced the CI, meaning a better stabilization of the emulsions was induced. The ChNF emulsions demonstrated better ability at emulsion stabilization than ChNC emulsions at the same concentrations, especially for ChNF concentrations greater than 0.8 wt% (Fig. 7(c)). Similar improvement to creaming stability for Pickering emulsions with increasing chitin nanoparticle concentrations has been observed (Tzoumaki et al., 2011). Moreover, the effect of concentration on the CI of ChNCs in Pickering emulsions was not as significant as the effect of ChNF concentrations. For example, the CIs of emulsions stabilized by ChNC concentrations of 0.1 wt % and 0.8 wt% after 42 days were 76.6% and 69.3%, respectively, whereas those of emulsions stabilized by ChNFs at the same concentrations were 61.28% and 11.6%, respectively.

Images of freshly prepared emulsions and those after a storage time of 42 days are shown in Fig. 7(d). We observed that creaming occurred in all ChNC emulsions, which suggested that the overall density of emulsion droplets was lower than that of water (Zhang, Chen et al., 2015; Zhang, Liu et al., 2015). In contrast, a thin oil layer was observed on the top of emulsions prepared with ChNC concentrations from 0.1 wt % to 0.4 wt%; this phenomenon is referred to as "oiling off" (McClements, 2007). This behavior is related to coalescence that may take place at low concentrations of chitin nanoparticles. It has been reported that particle concentrations affect the extent of coalescence during emulsification of solid-stabilized emulsions; in fact, the coalescence can be reduced by increasing the number of chitin nanoparticles in emulsions, which allows for the formation of networks of aggregated particles in the continuous phase, reducing the number of emulsion droplet collisions by providing a physical barrier against coalescence (Binks & Whitby, 2004; Mwangi et al., 2016; Tzoumaki et al., 2011). However, creaming of emulsions stabilized by ChNFs occurred for emulsions prepared with concentrations below 1 wt%. The emulsions stabilized by 1 wt% ChNFs showed slight creaming after 23 of days storage, whereas that stabilized by 1.4 wt% ChNFs exhibited no distinct creaming throughout the storage time.

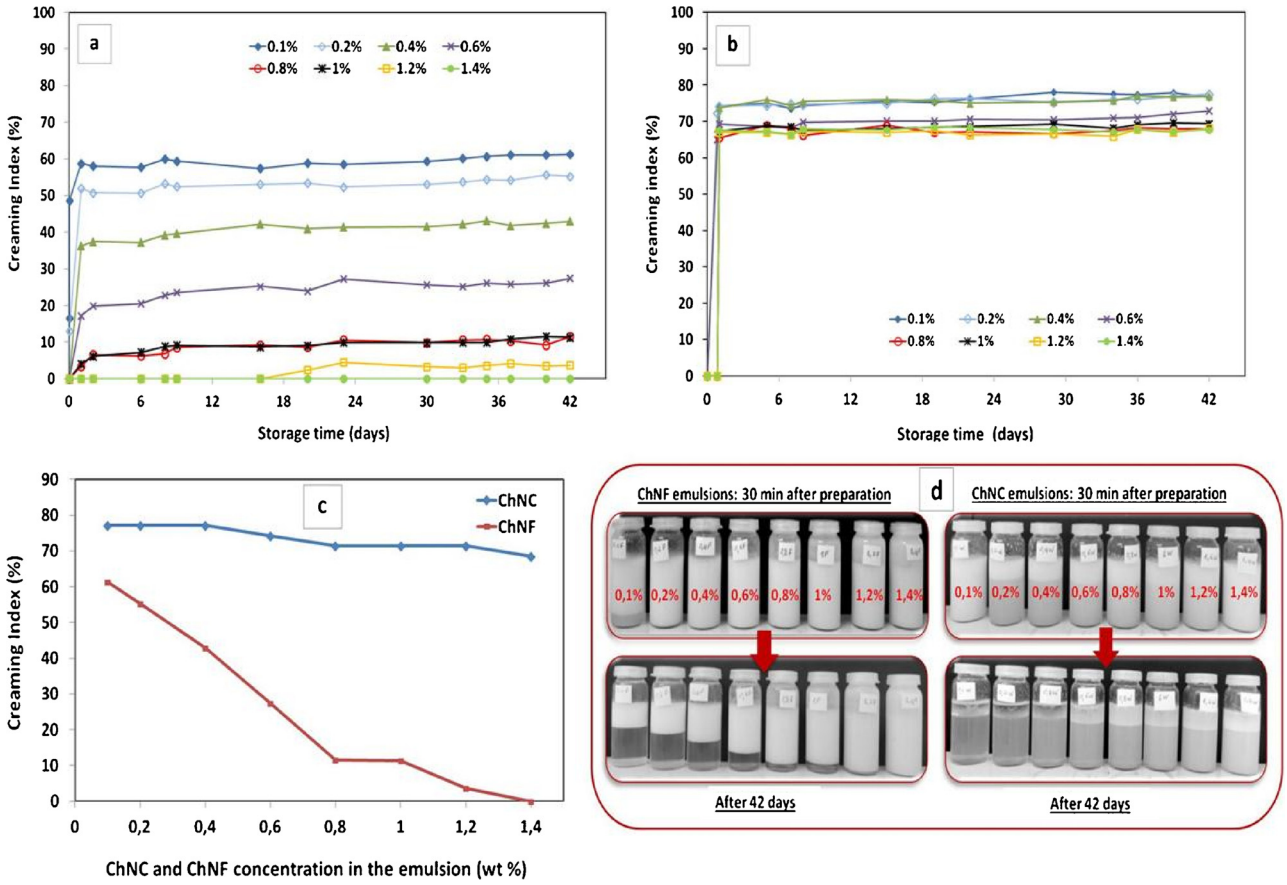

Fig. 7. Evolution of CI with storage time for different emulsions of (a) ChNFs and (b) ChNCs. Final CIs of emulsions after 42 days of storage (c) and photos of changes of emulsions taken on the day of preparation and after 42 days of storage (d).

3.5. Cytotoxicity of chitin nanomaterials

The studied chitin nanomaterials seem promising for some applications such as rheology modifiers or emulsion preparation. It was therefore appropriate to check if they present any cytotoxicity. To our knowledge, this is the first time that such characterization has been proposed. Extracts prepared from ChNCs and ChNFs did not indicate in vitro cytotoxicity to fibroblast-like and epithelial-like cells. The viability of the MDCK and MDCK-SIAT epithelial-like cells (Fig. 8(a) and (b), respectively), and the viability of Cos-1 and Cos-7 fibroblast-like cells (Fig. 8(c) and (d), respectively) that grew in the presence of different concentrations of ChNC and ChNF extracts (in the range of 0.15–10% w/v) were similar ($p > 0.05$) to the percent viability of their respective controls or cells grown in the presence of medium alone, corresponding to the 0% dose.

These results are clearly indicated in the morphological analysis of the cells exposed to extracts of ChNCs and ChNFs in Fig. 9, which shows the morphology of MDCK and Cos-7 cells as representatives of epithelial-like and fibroblast-like cells, respectively. In the case of epithelial-like MDCK cells, their characteristic polarization showed the formation of a monolayer with intimately connected cells (Fig. 9(a)–(c)); it is evident that the extracts of ChNCs and ChNFs did not have toxic components that could alter the integrity of cells grown in the monolayer. Similarly, the growth of Cos-7 cells of the fibroblast-like type in the presence of extracts of ChNCs and ChNFs (Fig. 9(e) and (f), respectively) occurred in similar way as the control (Fig. 9(d)). These fibroblast-like cells had growth in clusters and the cells were bound by cytoplasmic extensions such as lamellipodia and filopodia. Thus, the morphological and quantitative evidence of the growth of fibroblast-like and epithelial-like cells showed that both the ChNCs and the ChNFs prepared in this study did not show any cytotoxic effect for in vitro-cultured cells.

3.6. Process and energy comparison

The studied nanopolysaccharides possess interesting properties depending on their preparation procedure, and they are not cytotoxic. This is encouraging but not entirely sufficient for further utilization. Indeed, recent studies have mainly focused on the preparation and applications of ChNFs and ChNCs, but there are no published data from a process engineering and economic standpoint on the cost of production of such nanomaterials. Here, we provide information about the production cost of each nanomaterial using process engineering simulation. In Fig. 10, water, chemical, and energy requirements and associated costs are shown (see also Table S1 in Supplementary Data). The simulation of the purification process (Fig. 10(a)) revealed that huge amounts of chemicals and energy were consumed per kilogram of chitin (3.628 kg and 17.64 kW, respectively). Because of long pretreatment times (up to 6 h) at moderate temperature (80–100 °C) and use of expensive reactants, new chitin purification techniques should be developed for future industrial up-scaling. The ChNF preparation process (Fig. 10(b)) had a low water and chemical burden (0.066 m^3 and 0.112 kg, respectively), and the cost incurred by mechanical defibrillation would be admissible at the evaluated production scale (0.045 €/kg chitin). For high–production-capacity mills, this issue could be considered determinant regarding economic suitability/viability studies (Fan et al., 2012; Qing et al., 2013). Considering the ChNC production process (Fig. 10(c)), water requirements comprised 34% of the related total process cost (5.457 €/kg of initial chitin). As in the conventional nanocrystal production process (Goodrich & Winter, 2007;

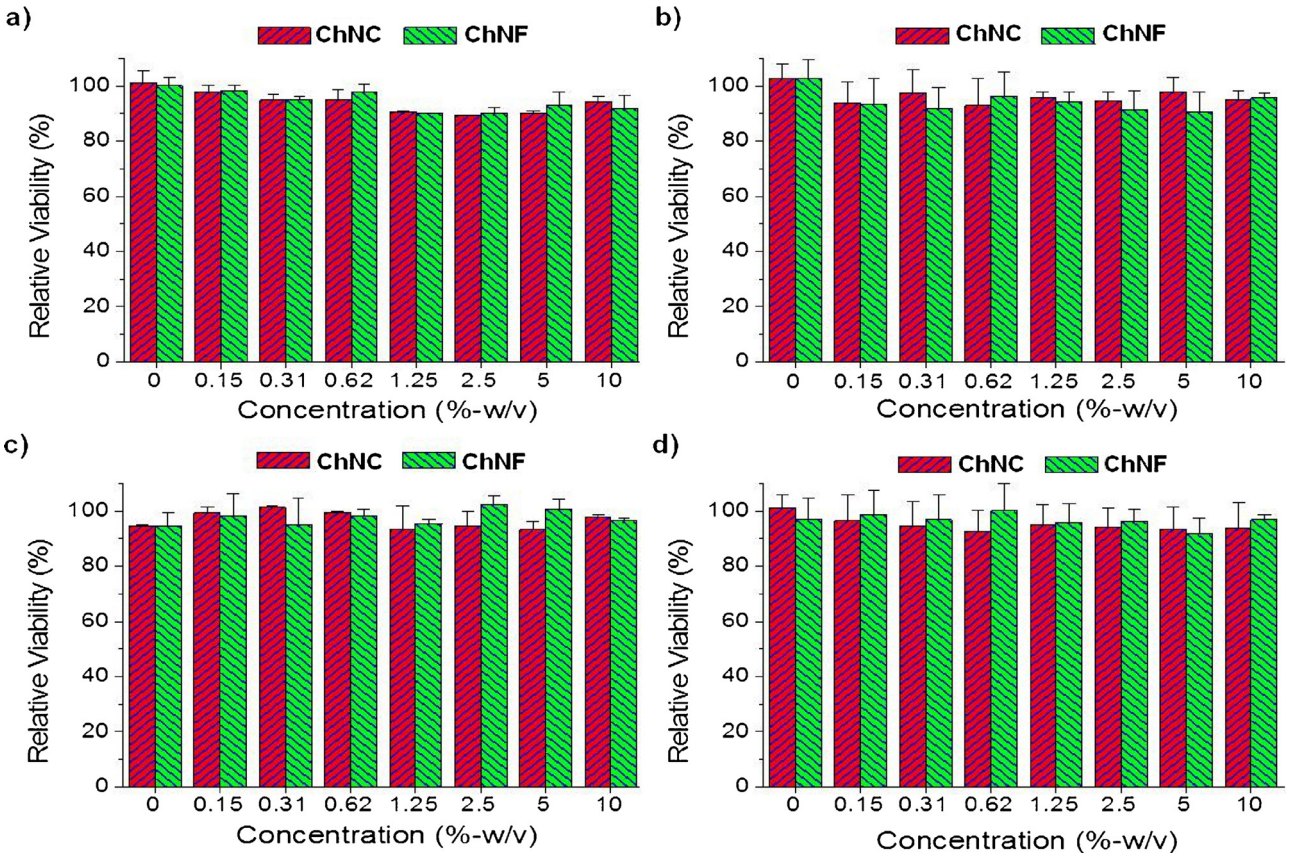

Fig. 8. In vitro cell growth in presence of different concentrations of ChNC and ChNF extracts. (a) MDCK, (b) MDCK-SIAT, (c) Cos-1, and (d) Cos-7 cells. The control is the 0% concentration.

Novo et al., 2015), energy consumption was moderate (9.741 kW/kg of initial chitin), but large amounts of acid (8.610 kg HCl/kg of initial chitin) and water for washing (2.096 m^3/kg chitin) were required. Thus, considering the simulation results, an economic estimation can be performed for ChNC and ChNF production, respectively, yielding 11.893 € and 6.688 € per kilogram of initial chitin. These values may appear high, but they become reasonable if we consider that there is still room for optimization and that price of nanopolysaccharides, like nanocellulose, is in the same range or even higher. Large-scale production of ChNFs seems to be the most promising strategy for further developments.

4. Conclusion

ChNCs and ChNFs were successfully extracted from similar commercial shrimp shell α-chitin. The properties of nanodispersions and their cast films were characterized. The average widths and lengths of ChNFs were (8.7 ± 3.2) nm and (673.9 ± 263.3) nm, respectively,

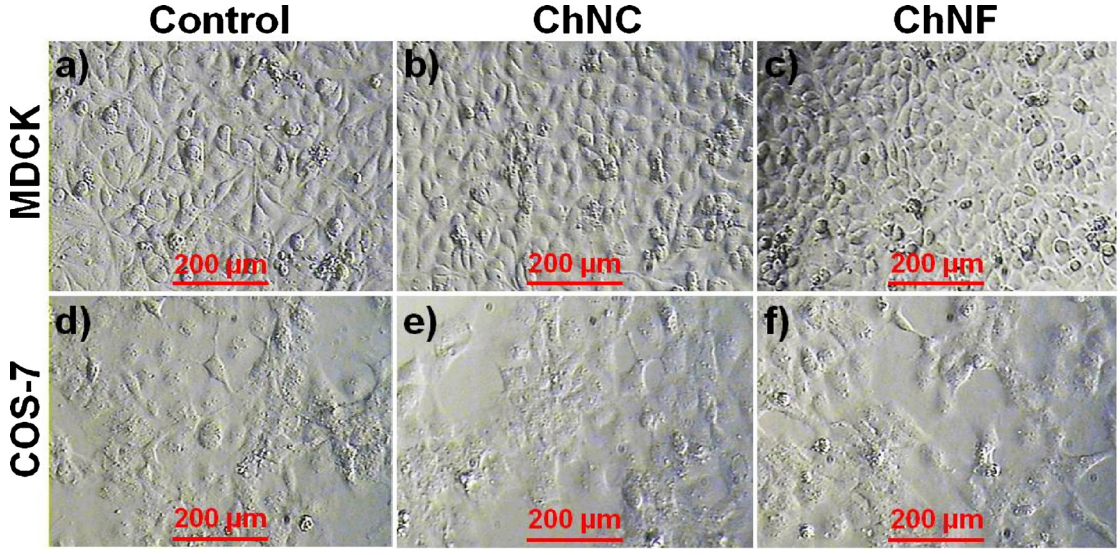

Fig. 9. Optical microscopy images showing the morphology of in vitro cell growth: (a)–(c) epithelial-like MDCK cells and (d)–(f) fibroblast-like Cos-7 cells.

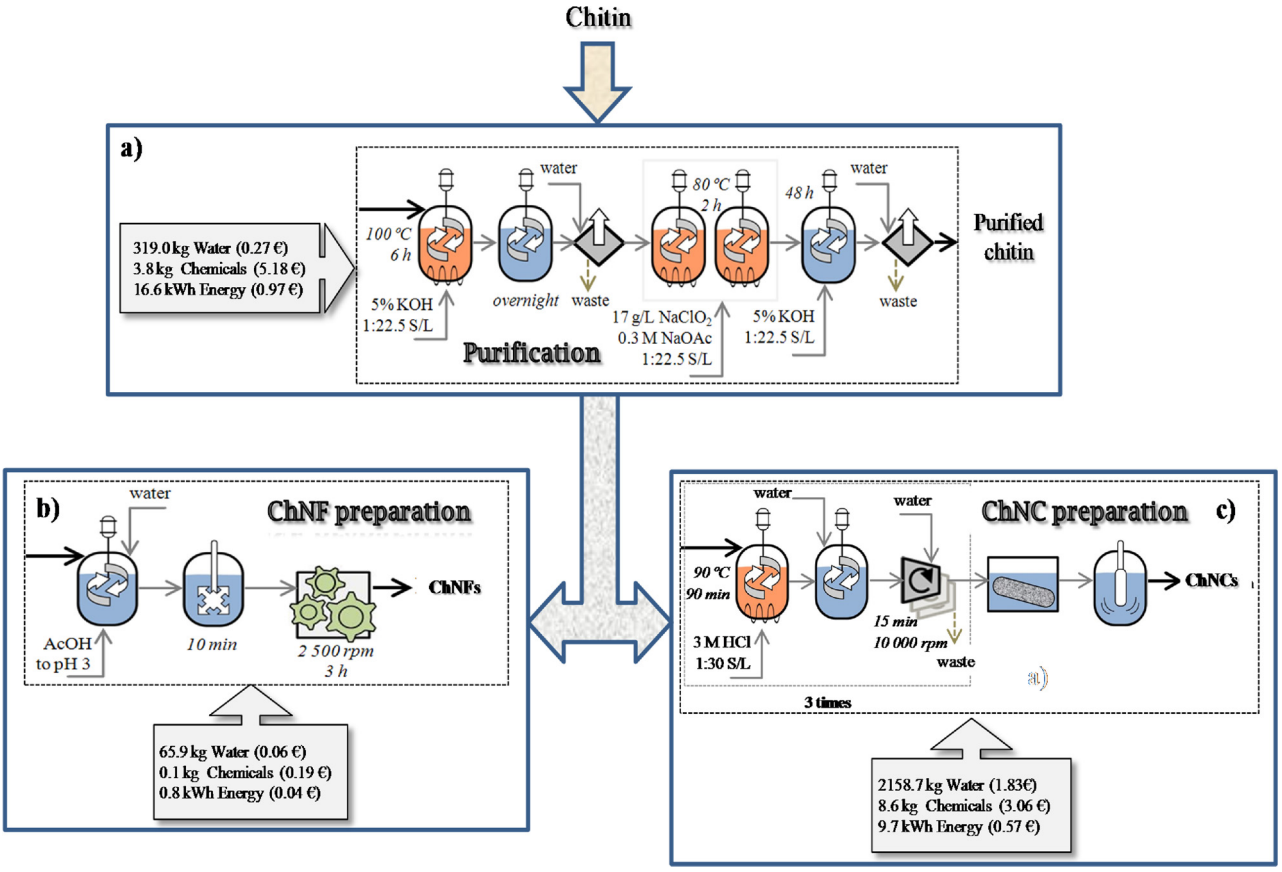

Fig. 10. Schematic diagram displaying the processes (i.e., main considered steps, conditions, and streams) and the required amounts and costs of water, chemicals, and energy per kg of initial chitin for (a) purification, (b) ChNF production, and (c) ChNC production.

whereas those for ChNCs were (9.7 ± 3.2) nm and (243.5 ± 55.1) nm, respectively. The casting film obtained from ChNCs exhibited high transparency but lower mechanical properties than ChNF film; thus, ChNFs offer superior nanomaterial reinforcing performance to ChNCs. The studies on rheological and emulsion properties indicated clear correlations to the aspect ratios and sizes of nanomaterials. In fact, ChNFs, which were longer and more flexible than ChNCs, displayed better Pickering emulsion stabilization ability and higher viscosity than ChNCs. The cytotoxicity data generated in this study showed for the first time that chitin nanomaterials had no toxic effect on epithelial and fibroblast cells, which suggests the possibility of their use in biological, medical, and food applications. A process engineering simulation was used to evaluate the energy and chemical consumption for each process of production, which demonstrated the lower cost, energy consumption, and simpler manufacturing facility for ChNFs compared to ChNCs. Overall, aside from the transparency of ChNC films, ChNFs had superior performance in all considered aspects.

Acknowledgements

Authors would like to thank the Spanish Ministry of Economy, Industry and Competitiveness (contract Juan de la Cierva Incorporacion IJCI-2015-23168).

References

Aklog, Y. F., Nagae, T., Izawa, H., Morimoto, M., Saimoto, H., & Ifuku, S. (2016). Preparation of chitin nanofibers by surface esterification of chitin with maleic anhydride and mechanical treatment. *Carbohydrate Polymers, 153*, 55–59.

Ang-atikarnkul, P., Watthanaphanit, A., & Rujiravanit, R. (2014). Fabrication of cellulose nanofiber/chitin whisker/silk sericin bionanocomposite sponges and characterizations of their physical and biological properties. *Composites Science and Technology, 96*, 88–96.

Binks, B. P., & Whitby, C. P. (2004). Silica particle-stabilized emulsions of silicone oil and water: Aspects of emulsification. *Langmuir, 20*(4), 1130–1137.

Butchosa, N., Brown, C., Tomas Larsson, P. A., Berglund, L., Bulone, V., & Zhou, Q. (2013). Nanocomposites of bacterial cellulose nanofibers and chitin nanocrystals: Fabrication, characterization and bactericidal activity. *Green Chemistry, 15*(12), 3404–3413.

Chappat, M. (1994). Some applications of emulsions. *Colloids and Surfaces A: Physicochemical and Engineering Aspects, 91*, 57–77.

Chen, J.-K., Shen, C.-R., & Liu, C.-L. (2010). N-Acetylglucosamine: Production and applications. *Marine Drugs, 8*(9), 2493–2516.

Cunha, A. G., Mougel, J.-B., Cathala, B., Berglund, L. A., & Capron, I. (2014). Preparation of double pickering emulsions stabilized by chemically tailored nanocelluloses. *Langmuir, 30*(31), 9327–9335.

Deng, Q., Li, J., Yang, J., & Li, D. (2014). Optical and flexible α-chitin nanofibers reinforced poly(vinyl alcohol) (PVA) composite film: Fabrication and property. *Composites Part A: Applied Science and Manufacturing, 67*, 55–60.

Ding, B., Huang, S., Pang, K., Duan, Y., & Zhang, J. (2018). Nitrogen-enriched carbon nanofiber aerogels derived from marine chitin for energy storage and environmental remediation. *ACS Sustainable Chemistry & Engineering, 6*(1), 177–185.

Ezekiel Mushi, N., Butchosa, N., Zhou, Q., & Berglund, L. A. (2014). Nanopaper membranes from chitin–protein composite nanofibers—structure and mechanical properties. *Journal of Applied Polymer Science, 131*(7), 40121.

Fan, Y., Saito, T., & Isogai, A. (2008a). Chitin nanocrystals prepared by TEMPO-mediated oxidation of α-Chitin. *Biomacromolecules, 9*(1), 192–198.

Fan, Y., Saito, T., & Isogai, A. (2008b). Preparation of chitin nanofibers from squid pen β-Chitin by simple mechanical treatment under acid conditions. *Biomacromolecules, 9*(7), 1919–1923.

Fan, Y., Saito, T., & Isogai, A. (2010). Individual chitin nano-whiskers prepared from partially deacetylated α-chitin by fibril surface cationization. *Carbohydrate Polymers, 79*(4), 1046–1051.

Fan, Y., Fukuzumi, H., Saito, T., & Isogai, A. (2012). Comparative characterization of aqueous dispersions and cast films of different chitin nanowhiskers/nanofibers. *International Journal of Biological Macromolecules, 50*(1), 69–76.

Garcia, I., Azcune, I., Casuso, P., Carrasco, P. M., Grande, H.-J., Cabañero, G., ... Avgeropoulos, A. (2015). Carbon nanotubes/chitin nanowhiskers aerogel achieved by quaternization-induced gelation. *Journal of Applied Polymer Science, 132*(37), 42547.

Goodrich, J. D., & Winter, W. T. (2007). α-Chitin nanocrystals prepared from shrimp

shells and their specific surface area measurement. *Biomacromolecules, 8*(1), 252–257.
Gopalan Nair, K., & Dufresne, A. (2003). Crab shell chitin whisker reinforced natural rubber nanocomposites. 1. Processing and swelling behavior. *Biomacromolecules, 4*(3), 657–665.
Gopi, S., Pius, A., & Thomas, S. (2016). Enhanced adsorption of crystal violet by synthesized and characterized chitin nano whiskers from shrimp shell. *Journal of Water Process Engineering, 14*, 1–8.
Ifuku, S., & Saimoto, H. (2012). Chitin nanofibers: Preparations, modifications, and applications. *Nanoscale, 4*(11), 3308–3318.
Ifuku, S., Nogi, M., Abe, K., Yoshioka, M., Morimoto, M., Saimoto, H., et al. (2009). Preparation of chitin nanofibers with a uniform width as α-Chitin from crab shells. *Biomacromolecules, 10*(6), 1584–1588.
Ifuku, S., Nogi, M., Abe, K., Yoshioka, M., Morimoto, M., Saimoto, H., & Yano, H. (2011). Simple preparation method of chitin nanofibers with a uniform width of 10–20 nm from prawn shell under neutral conditions. *Carbohydrate Polymers, 84*(2), 762–764.
Ifuku, S., Ikuta, A., Hosomi, T., Kanaya, S., Shervani, Z., Morimoto, M., & Saimoto, H. (2012). Preparation of polysilsesquioxane-urethaneacrylate copolymer film reinforced with chitin nanofibers. *Carbohydrate Polymers, 89*(3), 865–869.
Ifuku, S., Suzuki, N., Izawa, H., Morimoto, M., & Saimoto, H. (2014). Surface phthaloylation of chitin nanofiber in aqueous media to improve dispersibility in aromatic solvents and give thermo-responsive and ultraviolet protection properties. *RSC Advances, 4*(37), 19246–19250.
Ito, I., Osaki, T., Ifuku, S., Saimoto, H., Takamori, Y., Kurozumi, S., ... Minami, S. (2014). Evaluation of the effects of chitin nanofibrils on skin function using skin models. *Carbohydrate Polymers, 101*, 464–470.
Ji, Y., Wolfe, P. S., Rodriguez, I. A., & Bowlin, G. L. (2012). Preparation of chitin nanofibril/polycaprolactone nanocomposite from a nonaqueous medium suspension. *Carbohydrate Polymers, 87*(3), 2313–2319.
Julien, S., Chornet, E., & Overend, R. P. (1993). Influence of acid pretreatment (H2SO4, HCl, HNO3) on reaction selectivity in the vacuum pyrolysis of cellulose. *Journal of Analytical and Applied Pyrolysis, 27*(1), 25–43.
Kadokawa, J., Takegawa, A., Mine, S., & Prasad, K. (2011). Preparation of chitin nanowhiskers using an ionic liquid and their composite materials with poly(vinyl alcohol). *Carbohydrate Polymers, 84*(4), 1408–1412.
Kalashnikova, I., Bizot, H., Bertoncini, P., Cathala, B., & Capron, I. (2012). Cellulosic nanorods of various aspect ratios for oil in water Pickering emulsions. *Soft Matter, 9*(3), 952–959.
Kumirska, J., Czerwicka, M., Kaczyński, Z., Bychowska, A., Brzozowski, K., Thöming, J., et al. (2010). Application of spectroscopic methods for structural analysis of chitin and chitosan. *Marine Drugs, 8*(5), 1567–1636.
Laitinen, O., Ojala, J., Sirviö, J. A., & Liimatainen, H. (2017). Sustainable stabilization of oil in water emulsions by cellulose nanocrystals synthesized from deep eutectic solvents. *Cellulose, 24*(4), 1679–1689.
Li, M.-C., Wu, Q., Song, K., Cheng, H. N., Suzuki, S., & Lei, T. (2016). Chitin nanofibers as reinforcing and antimicrobial agents in carboxymethyl cellulose films: Influence of partial deacetylation. *ACS Sustainable Chemistry & Engineering, 4*(8), 4385–4395.
Li, J., Revol, J.-F., & Marchessault, R. H. (1996). Rheological properties of aqueous suspensions of chitin crystallites. *Journal of Colloid and Interface Science, 183*(2), 365–373.
Li, J., Revol, J.-F., Naranjo, E., & Marchessault, R. H. (1996). Effect of electrostatic interaction on phase separation behaviour of chitin crystallite suspensions. *International Journal of Biological Macromolecules, 18*(3), 177–187.
Liu, H., Liu, W., Luo, B., Wen, W., Liu, M., Wang, X., et al. (2016). Electrospun composite nanofiber membrane of poly(l-lactide) and surface grafted chitin whiskers: Fabrication, mechanical properties and cytocompatibility. *Carbohydrate Polymers, 147*, 216–225.
Liu, M., Zheng, H., Chen, J., Li, S., Huang, J., & Zhou, C. (2016). Chitosan-chitin nanocrystal composite scaffolds for tissue engineering. *Carbohydrate Polymers, 152*, 832–840.
Lu, Y., Sun, Q., She, X., Xia, Y., Liu, Y., Li, J., & Yang, D. (2013). Fabrication and characterisation of α-chitin nanofibers and highly transparent chitin films by pulsed ultrasonication. *Carbohydrate Polymers, 98*(2), 1497–1504.
Ma, H., Burger, C., Hsiao, B. S., & Chu, B. (2011). Ultrafine polysaccharide nanofibrous membranes for water purification. *Biomacromolecules, 12*(4), 970–976.
Ma, L., Liu, M., Peng, Q., Liu, Y., Luo, B., & Zhou, C. (2016). Crosslinked carboxylated SBR composites reinforced with chitin nanocrystals. *Journal of Polymer Research, 23*(7), 134.
McClements, D. J. (2007). Critical review of techniques and methodologies for characterization of emulsion stability. *Critical Reviews in Food Science and Nutrition, 47*(7), 611–649.
Mushi, N. E., Butchosa, N., Salajkova, M., Zhou, Q., & Berglund, L. A. (2014). Nanostructured membranes based on native chitin nanofibers prepared by mild process. *Carbohydrate Polymers, 112*, 255–263.
Muzzarelli, R. A. A., Morganti, P., Morganti, G., Palombo, P., Palombo, M., Biagini, G., ... Muzzarelli, C. (2007). Chitin nanofibrils/chitosan glycolate composites as wound medicaments. *Carbohydrate Polymers, 70*(3), 274–284.
Muzzarelli, R. A. A., Boudrant, J., Meyer, D., Manno, N., DeMarchis, M., & Paoletti, M. G. (2012). Current views on fungal chitin/chitosan, human chitinases, food preservation, glucans, pectins and inulin: A tribute to Henri Braconnot, precursor of the carbohydrate polymers science, on the chitin bicentennial. *Carbohydrate Polymers, 87*(2), 995–1012.
Muzzarelli, R. A. A. (1983). Chitin and its derivatives: New trends of applied research. *Carbohydrate Polymers, 3*(1), 53–75.
Mwangi, W. W., Ho, K.-W., Tey, B.-T., & Chan, E.-S. (2016). Effects of environmental factors on the physical stability of pickering-emulsions stabilized by chitosan particles. *Food Hydrocolloids, 60*, 543–550.
Noh, H. K., Lee, S. W., Kim, J.-M., Oh, J.-E., Kim, K.-H., Chung, C.-P., ... Min, B.-M. (2006). Electrospinning of chitin nanofibers: Degradation behavior and cellular response to normal human keratinocytes and fibroblasts. *Biomaterials, 27*(21), 3934–3944.
Novo, L. P., Bras, J., García, A., Belgacem, N., & Curvelo, A. A. S. (2015). Subcritical water: A method for green production of cellulose nanocrystals. *ACS Sustainable Chemistry & Engineering, 3*(11), 2839–2846.
Paillet, M., & Dufresne, A. (2001). Chitin whisker reinforced thermoplastic nanocomposites. *Macromolecules, 34*(19), 6527–6530.
Pang, K., Ding, B., Liu, X., Wu, H., Duan, Y., & Zhang, J. (2017). High-yield preparation of a zwitterionically charged chitin nanofiber and its application in a doubly pH-responsive Pickering emulsion. *Green Chemisry, 19*(15), 3665–3670.
Pangon, A., Saesoo, S., Saengkrit, N., Ruktanonchai, U., & Intasanta, V. (2016). Hydroxyapatite-hybridized chitosan/chitin whisker bionanocomposite fibers for bone tissue engineering applications. *Carbohydrate Polymers, 144*, 419–427.
Pereira, A. G. B., Muniz, E. C., & Hsieh, Y.-L. (2014). Chitosan-sheath and chitin-core nanowhiskers. *Carbohydrate Polymers, 107*, 158–166.
Perrin, E., Bizot, H., Cathala, B., & Capron, I. (2014). Chitin nanocrystals for pickering high internal phase emulsions. *Biomacromolecules, 15*(10), 3766–3771.
Phongying, S., Aiba, S., & Chirachanchai, S. (2007). Direct chitosan nanoscaffold formation via chitin whiskers. *Polymer, 48*(1), 393–400.
Qing, Y., Sabo, R., Zhu, J. Y., Agarwal, U., Cai, Z., & Wu, Y. (2013). A comparative study of cellulose nanofibrils disintegrated via multiple processing approaches. *Carbohydrate Polymers, 97*(1), 226–234.
Rahimi, M., Brown, R. J., Tsuzuki, T., & Rainey, T. (2016). A comparison of cellulose nanocrystals and cellulose nanofibres extracted from bagasse using acid and ball milling methods. Advances in Natural Sciences. *Nanoscience and Nanotechnology, 7*, 035004.
Revol, J.-F., & Marchessault, R. H. (1993). In vitro chiral nematic ordering of chitin crystallites. *International Journal of Biological Macromolecules, 15*(6), 329–335.
Rinaudo, M. (2006). Chitin and chitosan: Properties and applications. *Progress in Polymer Science, 31*(7), 603–632.
Salaberria, A. M., Labidi, J., & Fernandes, S. C. M. (2014). *Chitin nanocrystals and nanofibers as nano-sized fillers into thermoplastic starch-based biocomposites processed by melt-mixing*.
Salaberria, A. M., Fernandes, S. C. M., Diaz, R. H., & Labidi, J. (2015). Processing of α-chitin nanofibers by dynamic high pressure homogenization: Characterization and antifungal activity against A. niger. *Carbohydrate Polymers, 116*, 286–291.
Shankar, S., Reddy, J. P., Rhim, J.-W., & Kim, H.-Y. (2015). Preparation, characterization, and antimicrobial activity of chitin nanofibrils reinforced carrageenan nanocomposite films. *Carbohydrate Polymers, 117*, 468–475.
Sriupayo, J., Supaphol, P., Blackwell, J., & Rujiravanit, R. (2005). Preparation and characterization of α-chitin whisker-reinforced chitosan nanocomposite films with or without heat treatment. *Carbohydrate Polymers, 62*(2), 130–136.
Stawski, D., Rabiej, S., Herczyńska, L., & Draczyński, Z. (2008). Thermogravimetric analysis of chitins of different origin. *Journal of Thermal Analysis and Calorimetry, 93*(2), 489–494.
Tzoumaki, M. V., Moschakis, T., Kiosseoglou, V., & Biliaderis, C. G. (2011). Oil-in-water emulsions stabilized by chitin nanocrystal particles. *Food Hydrocolloids, 25*(6), 1521–1529.
Wang, W., Du, G., Li, C., Zhang, H., Long, Y., & Ni, Y. (2016). Preparation of cellulose nanocrystals from asparagus (Asparagus officinalis L.) and their applications to palm oil/water Pickering emulsion. *Carbohydrate Polymers, 151*, 1–8.
Wang, Q., Yan, X., Chang, Y., Ren, L., & Zhou, J. (2018). Fabrication and characterization of chitin nanofibers through esterification and ultrasound treatment. *Carbohydrate Polymers, 180*(Suppl. C), 81–87.
Wu, J., Lin, H., & Meredith, J. C. (2016). Poly(ethylene oxide) bionanocomposites reinforced with chitin nanofiber networks. *Polymer, 84*, 267–274.
Zeinali, E., Haddadi-Asl, V., & Roghani-Mamaqani, H. (2014). Nanocrystalline cellulose grafted random copolymers of N-isopropylacrylamide and acrylic acid synthesized by RAFT polymerization: Effect of different acrylic acid contents on LCST behavior. *RSC Advances, 4*(59), 31428–31442.
Zhang, Y., Chen, Z., Bian, W., Feng, L., Wu, Z., Wang, P., & Wu, T. (2015). Stabilizing oil-in-water emulsions with regenerated chitin nanofibers. *Food Chemistry, 183*, 115–121.
Zhang, Y., Jiang, J., Liu, L., Zheng, K., Yu, S., & Fan, Y. (2015). Preparation, assessment, and comparison of α-chitin nano-fiber films with different surface charges. *Nanoscale Research Letters,* 10.
Zhu, L., Liang, K., & Ji, Y. (2015). Prominent reinforcing effect of chitin nanocrystals on electrospun polydioxanone nanocomposite fiber mats. *Journal of the Mechanical Behavior of Biomedical Materials, 44*, 35–42.
Zuber, M., Zia, K. M., & Barikani, M. (2013). Chitin and chitosan based blends, composites and nanocomposites. In S. Thomas, P. M. Visakh, & A. P. Mathew (Eds.). *Advances in natural polymers* (pp. 55–119). Springer Berlin Heidelberg.